EasyChair Preprint

№ 5761

3D Analysis of Film Thickness Distribution in a Horizontal Type Falling Film Evaporator

Furqan Tahir, Abdelnasser Mabrouk and Muammer Koc

June 9, 2021

3D Analysis of Film Thickness Distribution in a Horizontal Type Falling Film Evaporator

[1*]Furqan Tahir, [1,2]Abdelnasser Mabrouk, [1]Muammer Koç
[1] Division of Sustainable Development (DSD), College of Science & Engineering (CSE), Hamad Bin Khalifa University (HBKU), Education City, P.O. Box 34110, Qatar
[2] Qatar Environment and Energy Research Institute (QEERI), Hamad Bin Khalifa University (HBKU), Education City, P.O. Box 34110, Qatar

* E-mails: futahir@hbku.edu.qa

Abstract
The film thickness characterization in the horizontal type falling film evaporators have been the primary focus of research in the past decade. Several experimental and numerical studies have been carried out to analyze film thickness distribution around horizontal tube. Because of experimental setup limitations, thickness measurements on complete tube area are not conceivable. However, numerical studies allow researchers to characterize falling film under flexible operating conditions. Present study focuses on quantification of film thickness distribution around horizontal tube in a three dimensional domain. Two tubes of 25.4 mm diameter have been selected for the computational fluid dynamics (CFD) simulations, with an orifice of 2x1 mm^2, an impingement height of 2 mm and an inter-tube spacing of 7.6 mm. The tube section of 22 mm has been opted as per critical wavelength formulation/distance between droplet sites. In order to reduce computational efforts, only quarter of the domain is considered for numerical calculations. The CFD model has been established in Ansys fluent v18.0 and has been validated quantitatively against Nusselt correlation and qualitatively with the experimental data available in the literature. The film thicknesses at different axial positions z = 0, 5.5 and 11 mm have been computed and compared and results show higher film thickness distribution at z = 0 mm (in line with droplet formation site) as compared to that of z = 11 mm (halfway between two droplet formation sites). The film thickness at θ = 90° is found to be 0.195 mm at z = 0 mm which is 21.1% higher than that of z = 11 mm.

Keywords: 3D, CFD, Falling Film, Film thickness, Horizontal Tube, Numerical Model

I. Introduction

The film thickness of the falling film exchangers have been studied experimentally by many researchers (Chen et al., 2015; Gstoehl et al., 2004; Hou et al., 2012). However, because of experimental limitations, thickness measurement at all locations is not possible. Therefore, employing numerical techniques to characterize film thickness distribution and hydrodynamics has been the primary focus in the past decade (Tahir et al., 2019a, 2019b, 2019c). Understanding falling film hydrodynamics would help in improving wettability, heat transfer coefficient and reducing scaling problems as these exchangers are commonly used in desalination and refrigeration industries (Mabrouk et al., 2017b, 2017a; Tahir et al., 2019d). In 1916, Nusselt (Nusselt, 1916) presented film thickness δ correlation, which is widely used till date and is expressed as:

$$\delta = \sqrt[3]{\frac{3\mu_l \Gamma_{1/2}}{\rho_l(\rho_l - \rho_g)g\sin\theta}} \quad (1)$$

where ρ is density, $\Gamma_{1/2}$ is liquid load (mass flow rate on one side of tube per unit tube length), μ is viscosity, θ is inclination angle, and g/l represents gas and liquid phases, respectively. Qiu et al. (Qiu et al., 2018) numerically studied the development of in-line and staggered jet mode. They found that trough is formed between the upstream jets in case of in-line mode and crest is formed in case of staggered mode. Tahir et al. (Tahir et al., 2021, 2020a, 2020b) investigated the effect of thermophysical properties on falling film hydrodynamics. They concluded that the higher surface tension and viscosity lead to higher film thickness that result in increased conduction thermal resistance that reduces the heat and mass transfer and hence the performance. Ding et al. (Ding et al., 2018) numerically examined the effect of wall adhesion on wettability and they noticed that the initial conditions significantly affects the wetted area. Furthermore, lower receding angle lead to improved wetting. Present work focuses on analyzing film thickness distribution in three-dimensional model. The computational fluid dynamics (CFD) model has been developed by discretizing conservation of mass and momentum equations for each phase, using volume of fluid (VOF) model (Tahir et al., 2018). A liquid load of 0.02 kg/(m·s) is considered for film thickness calculations, the results are compared with Nusselt solution and then film thickness distribution is analyzed and discussed.

II. Numerical model

Two tubes of 25.4 mm are selected for numerical calculations as shown in Fig.1a. The liquid enters from the 2x1 mm^2 with mass flow rate as boundary condition. The length of the section is chosen as 22 mm as per critical wavelength (Tahir et al., 2019a). In order to reduce computational efforts, only quarter of the geometry is considered due to symmetric nature. The liquid load $\Gamma_{1/2}$ is 0.02 kg/(m·s) that corresponds to the droplet mode. The thermophysical properties of water and water vapors are calculated at 20 °C. The liquid film falls under the action of gravity and without any vapor flow. The wall-adhesion contact angle is zero to ensure complete wetting (Khan et

al., 2019). The domain is meshed with hexahedral dominant elements as shown in Fig.1b. Fine boundary layers are provided adjacent to tube wall to capture liquid film accurately. The mass and momentum conservation equations for each phase are discretized using volume of fluid (VOF) model as shown in Eq. 2. The VOF model is widely used for multiphase flow problems that require distinct liquid phase interfaces (Baloch et al., 2018; Karmakar and Acharya, 2020).

$$\frac{\partial(\alpha_i \rho_i)}{\partial t} + \nabla \cdot \left(\alpha_i \rho_i \overrightarrow{V_i}\right) = 0 \qquad (i = g \ \ or \ \ l) \tag{2}$$

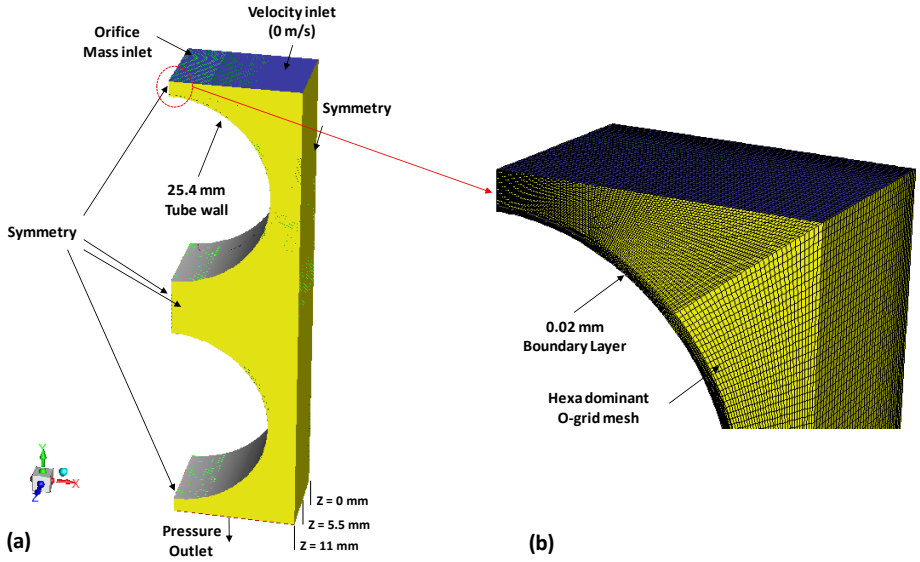

Fig. 1: (a) Domain with boundary conditions and (b) Hexahedral dominant mesh with fine boundary layers near to tube wall

where V represents velocity, α is volume fraction and g/l means gas/liquid phases. The surface tension and viscosity are computed by:

$$\beta = \alpha_l \beta_l + (1 - \alpha_l)\beta_g \tag{3}$$

where β represents any thermophysical property. The total number of elements are 562,575 and time step is 2 x 10^{-5} s after mesh and time dependency check, respectively.

III. Results and discussion

Fig.2 shows the comparison of CFD results and Nusselt solution (Eq.1), the CFD model agrees well in the range of θ = 30° - 150°. The film thickness from CFD deviates from Eq.1, in impingement and detachment regions because of inertial effects that are unaccounted in Eq.1. The water spreading on the tube at different time steps is shown in Fig.3. At t = 0.1 s, the water hits the tube surface and disperse in circumferential and axial direction under the action of gravity. The dispersion of water forms a thin liquid film on the tube surface. From t = 0.15 s to 0.25, it can be seen that the water moves faster at z = 0 mm plane as compared to other axial positions, which is in the same plane of orifice center. At t = 0.3 s, the water film reaches the tube bottom and starts compiling, the viscous and surface tension forces prevent it from falling. At the this moment, the tube is not fully wet and the liquid spreads in the axial direction from t = 0.3 s to 0.5 s. At t = 0.6 s, the tube is completely covered by liquid and the liquid keeps on gathering at the bottom forming departure sites. The liquid detaches as the gravitational force overcomes other forces.

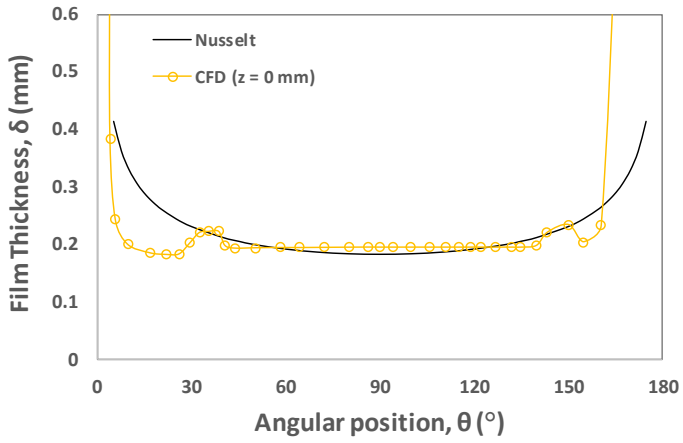

Fig. 2: Comparison between film thickness from CFD and Nusselt (Nusselt, 1916) solution for $\Gamma_{1/2}$ = 0.02 kg/(m·s)

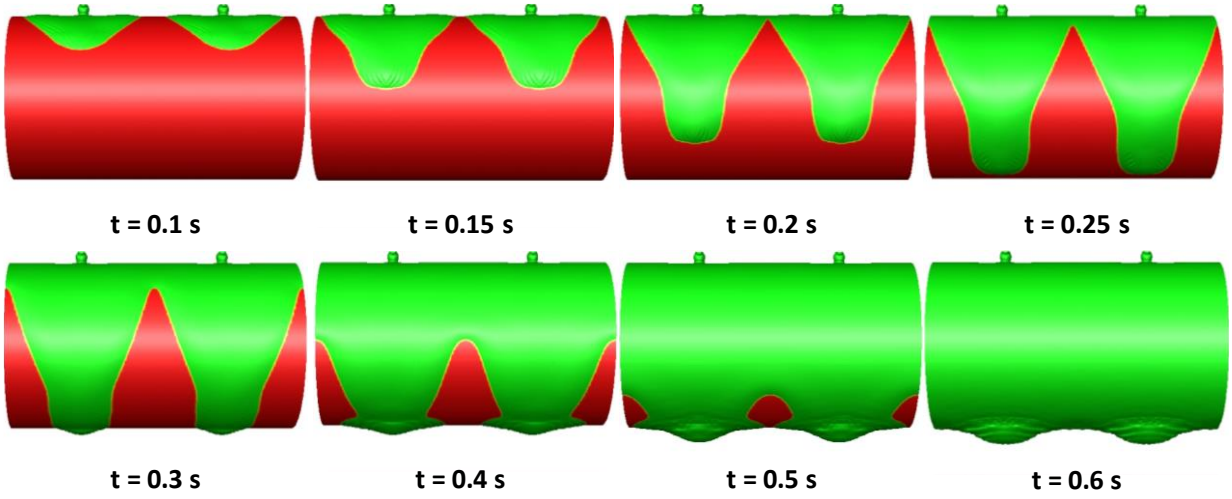

Fig. 3: Tube wetting at different time steps

Fig 4a shows the film thickness distribution around the tube circumference at different planes on axial direction. Three planes at z = 0 mm, 5.5 mm and 11 mm are selected for comparison purposes. The z = 0 mm plane lie in the center of orifice, whereas the z = 11 mm lie halfway between two droplet formation sites. At z = 0, the film thickness is found to be high as the continuous stream from orifice hits the tube surface, however far the impingement zone (z = 5.5 mm and 11 mm), the film thicknesses are low and found to be comparable. In most of the region, the film thickness is in the range of 0.15 – 0.3 mm. The minimum thickness is found at θ = 90° at z = 11 mm. Furthermore, the film thicknesses at different planes are found to be higher at the bottom region of the tube because of liquid accumulation. Fig 4b shows the film thickness variation in the axial direction form z = 0 mm to z = 11 mm at θ = 90°. It can be observed that the film thickness remains unchanged until z = 6 mm and after that it decreases as it is far from the droplet site plane. The film thickness is found to be 0.195 mm at z = 0 mm which is 21.1% higher than that of z = 11 mm.

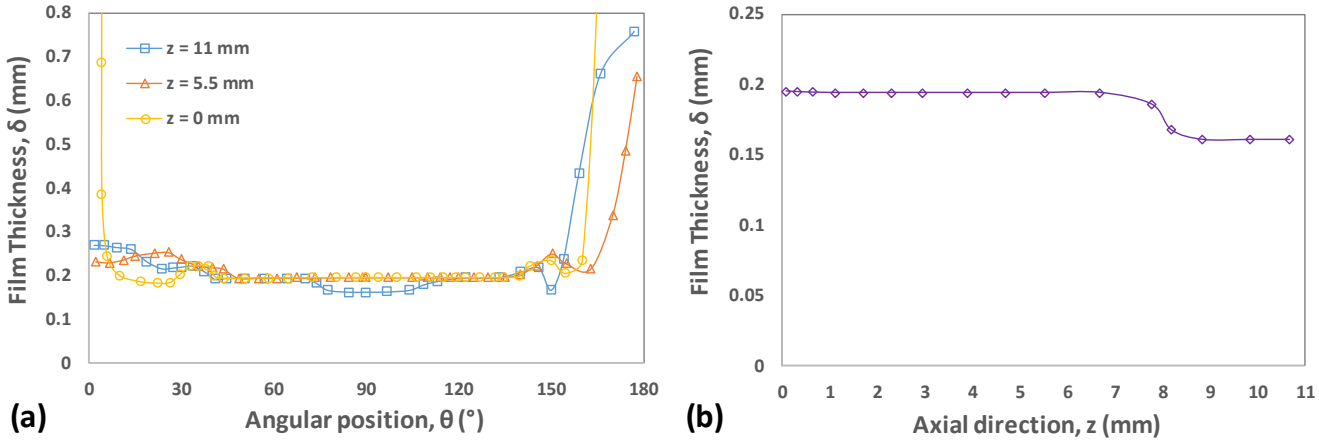

Fig. 4: (a) Film thickness distribution around the tube at different axial positions and (b) film thickness variation in the axial direction at an angular position of θ = 90°

IV. Conclusions

A three dimensional CFD model has been developed in Ansys fluent v18.0. The volume of fluid (VOF) model has been opted for liquid-gas interface tracking. The CFD model has been validated with the Nusselt solution, which is found in good agreement. The Nusslet solution does not accommodate inertial effects and because of this, variation in film thickness has been found in the top and bottom region of tube. As the liquid falls over the tube it moves quickly in the downward direction as compared to axial direction. The liquid film reaches the bottom at t = 0.3 s, however the complete wetting is achieved at t = 0.6 s. The film thickness is found between 0.15 – 0.3 mm, in most of the region and the minimum thickness is found at θ = 90°. In addition, the film thickness at the bottom is found to higher because of water accumulation. As the liquid moves farther from droplet site plane at θ = 90°, the film thickness gets thin. The film thickness and hydrodynamics study can be useful in evaluating conduction thermal resistance (film thickness/thermal conductivity) of liquid film, which can be used in predicting heat and mass transfer.

References

Baloch, A., Ali, H., Tahir, F., 2018. Transient Analysis of Air Bubble Rise in Stagnant Water Column Using CFD, in: ICTEA: International Conference on Thermal Engineering.

Chen, X., Shen, S., Wang, Y., Chen, J., Zhang, J., 2015. Measurement on falling film thickness distribution around horizontal tube with laser-induced fluorescence technology. Int. J. Heat Mass Transf. 89, 707–713. https://doi.org/10.1016/j.ijheatmasstransfer.2015.05.016

Ding, H., Xie, P., Ingham, D., Ma, L., Pourkashanian, M., 2018. Flow behaviour of drop and jet modes of a laminar falling film on horizontal tubes. Int. J. Heat Mass Transf. 124, 929–942. https://doi.org/10.1016/j.ijheatmasstransfer.2018.03.111

Gstoehl, D., Roques, J.F., Crisnel, P., Thome J. R., 2004. Measurement of Falling Film Thickness Around a Horizontal Tube Using a Laser Measurement Technique. Heat Transf. Eng. 25, 28–34. https://doi.org/10.1080/01457630490519899

Hou, H., Bi, Q., Ma, H., Wu, G., 2012. Distribution characteristics of falling film thickness around a horizontal tube. Desalination 285, 393–398. https://doi.org/10.1016/j.desal.2011.10.020

Karmakar, A., Acharya, S., 2020. Wettability Effects on Falling Film Flow and Heat Transfer Over Horizontal Tubes in Jet Flow Mode. J. Heat Transfer 142. https://doi.org/10.1115/1.4048088

Khan, S.A., Tahir, F., Baloch, A.A.B., Koc, M., 2019. Review of Micro–Nanoscale Surface Coatings Application for Sustaining Dropwise Condensation. Coatings 9, 117. https://doi.org/10.3390/coatings9020117

Mabrouk, A., Abotaleb, A., Abdelrehim, H., Tahir, F., Koc, M., Abdelrashid, A., Nasralla, A., 2017a. HP MED Plants, Part II: Novel Integration MED-Absorption Vapor Compression, in: IDA 2017 World Congress on Water Reuse and Desalination. Sao Paulo, Brazil.

Mabrouk, A., Abotaleb, A., Tahir, F., Darwish, M., Aini, R., Koc, M., Abdelrashid, A., 2017b. High Performance MED Desalination Plants Part I: Novel Design MED Evaporator, in: IDA 2017 World Congress on Water Reuse and Desalination. Sao Paulo, Brazil.

Nusselt, W., 1916. Die oberflachenkondensation des wasserdamphes. VDI-Zs 60, 541–546.

Qiu, Q., Zhang, X., Quan, S., Zhu, X., Shen, S., 2018. 3D numerical study of the liquid film distribution on the surface of a horizontal-tube falling-film evaporator. Int. J. Heat Mass Transf. 124, 943–952. https://doi.org/10.1016/j.ijheatmasstransfer.2018.04.020

Tahir, F., Mabrouk, A., Koc, M., 2019a. Review on CFD analysis of horizontal falling film evaporators in multi effect desalination plants. Desalin. Water Treat. 166, 296–320. https://doi.org/10.5004/dwt.2019.24487

Tahir, F., Mabrouk, A., Koc, M., 2019b. CFD Modeling of Falling Film Heat Transfer Over Horizontal Tube for Multi-Effect Desalination (MED) Evaporator, in: 1st International Conference on Sustainable Energy-Water-Environment Nexus In Desert Climate, Doha, Qatar.

Tahir, F., Mabrouk, A., Koc, M., 2019c. Heat Transfer Performance of Falling Film Evaporators Used in Multi Effect Desalination (MED) Plants, in: 1st International Conference on Sustainable Energy-Water-Environment Nexus In Desert Climate, Doha, Qatar.

Tahir, F., Mabrouk, A., Koc, M., 2019d. Energy and exergy analysis of thermal vapor compression (TVC) and absorption vapor compression (AVC) for multi effect desalination (MED) plants, in: 8th Global Conference on Global Warming (GCGW), Doha, Qatar. p. 25.

Tahir, F., Mabrouk, A., Koc, M., 2018. CFD Analysis of Falling Film Wettability in MED Desalination plants, in: Qatar Foundation Annual Research Conference Proceedings. p. EEPD650. https://doi.org/10.5339/qfarc.2018.EEPD650

Tahir, F., Mabrouk, A., Koç, M., 2021. Influence of co-current vapor flow on falling film over horizontal tube. Int. J. Therm. Sci. 159, 106614. https://doi.org/10.1016/j.ijthermalsci.2020.106614

Tahir, F., Mabrouk, A., Koç, M., 2020a. CFD Analysis of Falling Film Hydrodynamics for a Lithium Bromide (LiBr) Solution over a Horizontal Tube. Energies 13, 307. https://doi.org/10.3390/en13020307

Tahir, F., Mabrouk, A., Koç, M., 2020b. Impact of surface tension and viscosity on falling film thickness in multi-effect desalination (MED) horizontal tube evaporator. Int. J. Therm. Sci. 150, 106235. https://doi.org/10.1016/j.ijthermalsci.2019.106235